

Advancing Object Goal Navigation through LLM-enhanced Object Affinities Transfer

Mengying Lin, Shugao Liu, Dingxi Zhang, Yaran Chen*, Haoran Li, Dongbin Zhao

Abstract—In object goal navigation, agents navigate towards objects identified by category labels using visual and spatial information. Previously, solely network-based methods typically rely on historical data for object affinities estimation, lacking adaptability to new environments and unseen targets. Simultaneously, employing Large Language Models (LLMs) for navigation as either planners or agents, though offering a broad knowledge base, is cost-inefficient and lacks targeted historical experience. Addressing these challenges, we present the LLM-enhanced Object Affinities Transfer (LOAT) framework, integrating LLM-derived object semantics with network-based approaches to leverage experiential object affinities, thus improving adaptability in unfamiliar settings. LOAT employs a dual-module strategy: a generalized affinities module for accessing LLMs’ vast knowledge and an experiential affinities module for applying learned object semantic relationships, complemented by a dynamic fusion module harmonizing these information sources based on temporal context. The resulting scores activate semantic maps before feeding into downstream policies, enhancing navigation systems with context-aware inputs. Our evaluations conducted in the AI2-THOR and Habitat simulators indicate significant improvements in both navigation success rates and overall efficiency. Furthermore, the system performs effectively when deployed on a real robot without requiring additional training, thereby validating the efficacy of LOAT in integrating LLM insights for enhanced object-goal navigation.

Index Terms—Object Goal Navigation, Commonsense Reasoning, Generalization

I. INTRODUCTION

Object goal navigation is a significant area of study that focuses on enabling intelligent agents to navigate to a specified target object within a scene given category names. The objective is not only to successfully navigate to the object, but also to minimize the navigation path [1], [2]. To make the searching process successful and more efficient, researchers have explored how to leverage object semantic relationships in household environment to assist in information filtering for more efficient navigation.

Some researchers [3] explore non-training methods to discern these relationships, calculating Euclidean distances between object categories as a proxy for semantic proximity. However, this approach falls short in accurately reflecting navigable path lengths, especially in complex layouts like

multi-room settings. In such scenarios, objects that are geographically close in Euclidean terms might be practically separated by barriers such as walls, misleading the navigation process.

Deep learning methods offer alternative strategies for modeling object relationships. Zhang et al. introduce the hierarchical object-to-zone (HOZ) [4] graph for coarse-to-fine navigation guidance. Dang et al. propose the directed object attention (DOA) graph [5], explicitly modeling attention relationships. Li et al. develop the Class-Independent Relationship Network (CIRN) [6], decoupling navigation from target features by not relying on environmental cues. However, these graph-based approaches, which represent categories as nodes and their correlations as edges, struggle with generalizing due to inherent biases from training environments and fail to cope with unseen targets due to fixed nodes.

Models relying solely on training experiences often suffer from overfitting and tend to underperform when applied to novel environments or unfamiliar objects. To cope with that, some scholars are leveraging large models for richer object contextual insights to improve navigation system generalization. For instance, Zhou et. al [7] employs a pre-trained vision-language model (VLN) for open-world prompt-based positioning and a large language model to score object relevance numerically. Nonetheless, this method may face challenges like inconsistent inference scores and variable object priorities with paraphrased prompts, which could affect system stability. Empirical studies reveal that while LLMs may not deliver consistent scores across diverse prompts, they reliably identify relevant objects in a stable manner. Therefore, we focus on object relevance rather than the specific scores provided by LLMs to ensure a more consistent and reliable source of generalized knowledge.

Explorations into directly leveraging large models (LLMs or VLMs) as navigation agents like SayNav [8] and NavGPT [9] have shown promising results. However, the approach’s reliance on frequent and computationally intensive queries for each navigation step poses significant challenges, limiting its practicality due to high time and resource demands. Moreover, while these models are adept at general reasoning, their expansive knowledge base may lack the specificity needed for certain navigation contexts—such as culturally specific household layouts—potentially resulting in suboptimal navigational performance.

In this study, we present the LLM-enhanced Object Affinities Transfer (LOAT) framework (shown in Fig. 1), designed to augment robots’ adaptability and navigational capabilities in novel environments by integrating large language models’

*Corresponding author.

M. Lin, S. Liu, Y. Chen, H. Li, D. Zhao are with Institute of Automation, Chinese Academy of Sciences, Beijing. (e-mails: linnmengying20@mails.ucas.ac.cn, {liushugao2023, chenyan2013, dongbin.zhao}@ia.ac.cn)

M. Lin is with Georgia Institute of Technology, Atlanta, US. (e-mail: mlin365@gatech.edu)

D. Zhang is with ETH Zurich, Zurich, CH. (e-mail: zhangdi@ethz.ch)

TABLE I
COMPARISON OF NAVIGATION METHODS

Method	Traditional Navigation Methods		Network Agent w LOAT
	LM Agent/Planner	Network Agent	
Generalization	✓	✗	✓
Cost-efficient	✗	✓	✓
Stability	✗	✓	✓

(LLM) commonsense reasoning with historical experiences. The essence of LOAT is leveraging LLMs’ semantic understandings of object relationships to overcome the limitations of historical experiences in new settings while still keep the overall system cost effective.

This integration is realized by mathematically modeling the semantic relationships of objects through an attention mechanism, which is then utilized to activate the semantic maps. The framework comprises two pivotal submodules: the experiential affinities module for identifying past environmental patterns and a generalized affinities module focusing on LLM-identified relevant objects for enhanced generalization in new environments. A Dynamic Fusion Module carefully balances two sources of object affinities based on temporal contexts. The obtained weights are then applied to activate semantic maps for downstream policy. By utilizing experiential object affinities and the extensive semantic knowledge from LLMs, this approach integrates a context-aware navigation strategy by instructing models to concentrate on objects that are semantically related with the target, therefore heightening decision-making precision.

The LOAT framework boasts three key advantages:

- 1) **Dual-Module Framework Integration:** This work integrates commonsense reasoning from LLM with historical experiences, enhancing both efficiency and generalization. Commonsense knowledge is accessible at the beginning of each episode or stored offline for specific tasks, providing cost-effectiveness without compromising generalization.
- 2) **Utilization of Pretrained Text Embeddings:** By employing pretrained text embeddings for target representations, this approach decouples target identification from traditional one-hot encodings and environmental visuals. This ensures adaptability to unseen objects and enhances generalization beyond specific visual features.
- 3) **Performance Improvements in Navigation Policies:** The proposed method demonstrates significant performance enhancements across all semantic map-based navigation policies, from metric to topological maps, in simulations using Habitat [10] and AI2-THOR [11]. Furthermore, in empirical experiments, the system performs effectively when deployed on a real robot without requiring additional training, validating the efficacy of LOAT in integrating LLM insights for enhanced object-goal navigation.

II. RELATED WORK

A. Maps for Navigation

The field of mobile robot navigation has significantly benefited from advancements in Simultaneous Localization and Mapping (SLAM) [12], a technique essential for creating maps of unknown environments while concurrently determining the sensor system’s location. This dual capability is foundational for enabling autonomous navigation within these spaces.

Within SLAM research, two predominant mapping paradigms have emerged: metric based mapping and topological mapping. Metric based mapping methods [13]–[16], which generate detailed maps by aggregating neighboring pixels into a grid, are known for their precision. However, these methods may encounter challenges related to computational complexity, especially in large-scale indoor environments [17]. While these maps offer high accuracy, their dense representation of the environment can hinder efficient planning and problem-solving.

Conversely, topological mapping offers a more streamlined approach by depicting the environment through interconnected nodes, representing distinct landmarks or areas [4], [18]–[20]. This representation simplifies navigation and planning by abstracting the environment into a series of relationships between key locations. However, achieving accurate and consistent topological maps remains a challenge, especially in complex environments where sensor data may not consistently provide clear distinctions.

In this context, our study investigates the LOAT module’s efficacy in leveraging both metric and topological maps for navigation, showcasing its versatility across varying environmental representations.

B. Navigation with Large Models Integrated

Incorporating large models into navigation systems unfolds across three principal methodologies:

Object Relevance Scoring with Scripted Strategies: This approach leverages large models to evaluate object relevance, utilizing scripted search strategies such as frontier-based searching methods [21]. For instance, ESC [7] employs LLMs for direct candidate scoring, while L3MVN [22] and Prompter [23] derive collocation probabilities from masked language models with prompts like “Something you find at [MASK] is [TARGET],” scoring candidates based on their placement in the “[MASK]” token. However, the sensitivity of these models to subtle changes in language can result in significant variability in scores with slight prompt modifications, thereby affecting the consistency of object relevance assessments.

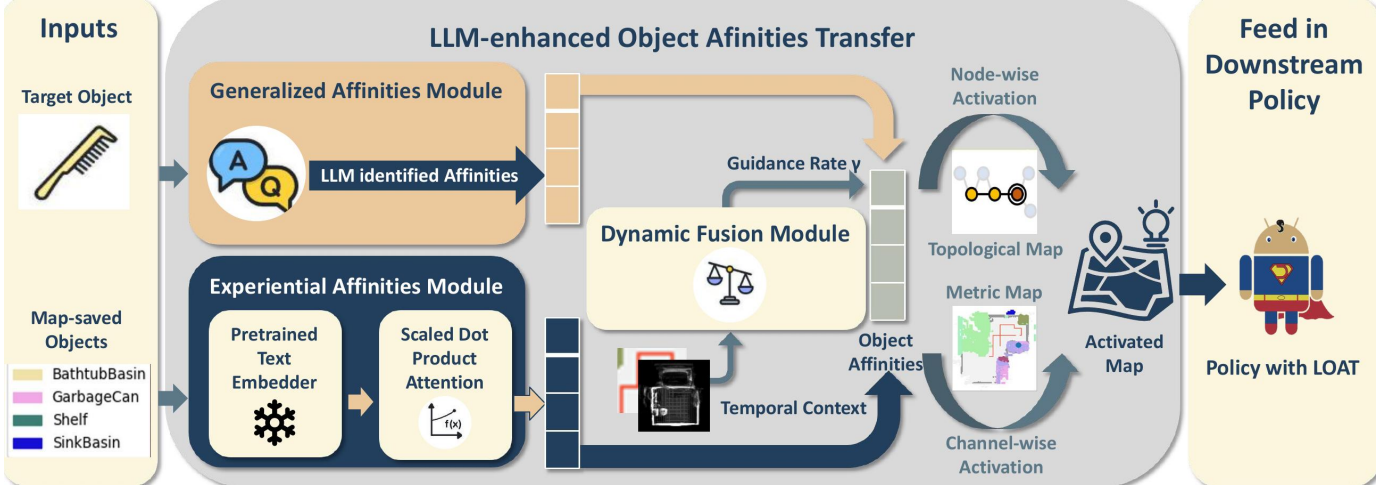


Fig. 1. **Detailed LOAT Framework.** In the LOAT framework, the target object and the categories of objects within the scene map are processed to determine the target location based on object affinities. Information about these categories is fed into two main modules. The Generalized Affinities Module, powered by LLMs, provides a normalized binary assessment of each object’s general relevance. Simultaneously, the Experiential Module utilizes a pretrained text embedder and key-query transformations to generate attention scores reflecting object affinities based on historical training data. These scores from both modules are then dynamically balanced by a fusion module that incorporates temporal state embeddings. Obtained scores are applied for node-wise or channel-wise activation depending on map categories before feeding downstream policy.

High-Level Planning with Large Models: Useful in long-horizon navigation tasks, this method involves using large models for strategic planning and task decomposition. For example, LLM-Planner [24] utilizes LLMs to break down tasks and identify key landmarks from instructions, establishing subgoals for navigation and initiating replanning upon failure. This strategy faces limitations in scenarios lacking explicit high-level instructions for targeting objects.

Direct Navigation Agent Utilization: Techniques like SayNav [8] and NavGPT [9] directly engage language models as navigational agents, necessitating frequent prompts at every step. While conceptually appealing for its dynamic adaptability, the practicality of this method is constrained by the associated computational and time costs, making it less feasible for wide-scale application.

III. METHODS

Instead of employing Large Language Models (LLMs) as high-level planners, which typically necessitates complex alignments with low-level policies, our approach enables the direct utilization of language-based priors in a numerical format that is intuitively interpretable to downstream models. As illustrated in Fig. 1, the LOAT framework merges LLM-derived commonsense insights with historical object affinity data to enhance semantic maps, effectively bridging the gap between high-level semantic understanding and low level network-based policy. This is achieved by feeding target object categories and environmental data into two sub-modules: the Generalized Affinities Module, which captures broad semantic knowledge from LLMs, and the Experiential Affinities Module, which leverages learned object relationship patterns from training data. A Dynamic Fusion Module dynamically balances these sources based on temporary contexts, improving the system adaptability and decision-making capabilities in unfamiliar environments. The obtained affinity scores are then

utilized for node-wise or channel-wise activation according to the map types. The enriched semantic map is then fed to downstream navigation policies for enhanced context-aware decision planning.

A. Experiential Affinities Module

This module aims at extracting object affinities from training time. It employs scaled dot-product attention to determine the relevance of each environmental object to the target object, leveraging pre-trained text embeddings. The set of objects in maps is represented as $\mathcal{O} = \{o_1, o_2, \dots, o_M\}$, where M is the total category number in maps and o_{target} is the target object. The embedding for any object o_i obtained through a pre-trained text embedder is $e(o_i)$.

To compute the attention scores, we first transform the embeddings into queries \mathbf{Q} and keys \mathbf{K} using learned linear transformations for the target object and all other objects respectively:

$$\mathbf{Q} = \mathbf{W}_q e(o_{target}), \quad \mathbf{K} = \mathbf{W}_k e(o_i), \quad (1)$$

where \mathbf{W}_q and \mathbf{W}_k are weight matrices for queries and keys.

The experiential attention score A_{E_i} for each object o_i is then calculated using the scaled dot-product of queries and keys:

$$A_{E_i} = \frac{\exp(\mathbf{Q} \cdot \mathbf{K}_j^T / \sqrt{d_k})}{\sum_{j=1}^M \exp(\mathbf{Q} \cdot \mathbf{K}_j^T / \sqrt{d_k})}, \quad (2)$$

where d_k is the dimensionality of the key vectors, serving to scale the dot product such that it leads to more stable gradients, with \mathbf{K}_j being the key corresponding to the j^{th} object in the environment.

This mechanism effectively captures the semantic relationship between the target object and every other object in the map by prioritizing objects based on the scaled similarity of their embeddings to the target. The resultant attention

scores guide the module to emphasize features from objects more closely related to the target in training experiences, thus enhancing pattern recognition and facilitating more informed navigation decisions within known contexts.

B. Generalized Affinities Module

The generalized affinities module leverages semantic relations derived from Large Language Models (LLMs) to enhance the model’s focus on objects semantically related to a specified target. While an intuitive approach might be to have these large models score object affinities directly, a key challenge emerges due to the inconsistency in inference scores and varied object priorities when prompting. Paraphrased prompts can lead to unstable and inconsistent scoring, potentially undermining the system’s reliability. To address this, we shift the focus from relying on specific scores to emphasizing object relevance, ensuring a more consistent and dependable source of generalized knowledge. Therefore, we use priors from large models solely as identifiers of relevant objects rather than for exact scoring. The semantic relevance of each object o_i in the map to the target o_{target} is determined by a binary value $S(o_i, o_{target})$, indicated by a LLM. This setup ensures that all objects deemed semantically related to the target are assigned a non-zero attention weight and remain unaffected by the object affinities from training data. By employing this uniform attention mechanism, the module guarantees that the agent considers all potentially relevant objects, thus improving its adaptability and performance in unfamiliar settings.

The generalized attention weight A_{G_i} for each object o_i is calculated as:

$$A_{G_i} = \frac{S(o_i, o_{target})}{\sum_{j=1}^M S(o_j, o_{target})}. \quad (3)$$

The final output of the generalized affinities module is a normalized vector, which directs the agent’s focus towards objects of interest specified by LLM for better generalization.

C. Dynamic Fusion Module

The dynamic fusion module synergizes the outputs from the generalized affinities module (A_G) and the experiential affinities module (A_E), finely tuning the balance between learned patterns and semantic guidance for optimal navigation performance. Specifically, it adjusts the contributions of A_{G_i} and A_{E_i} , the attention scores for an object o_i from the respective modules, ensuring an adaptive final attention mechanism.

This adaptation is driven by the guidance ratio γ , which is dynamically modulated based on the temporal context \mathcal{H} and, when available, additional environmental factors \mathcal{E} .

In architectures utilizing RNNs to encode the current state, \mathcal{H} includes the hidden states of the RNNs. For non-RNN architectures, \mathcal{H} encompasses the agent’s past trajectory and relevant environmental data, such as explored regions and observed layouts. \mathcal{E} further enriches this context with external cues, aiding in the precise adjustment of γ .

The key idea involves extracting features that capture historical and environmental contexts, with processing tailored

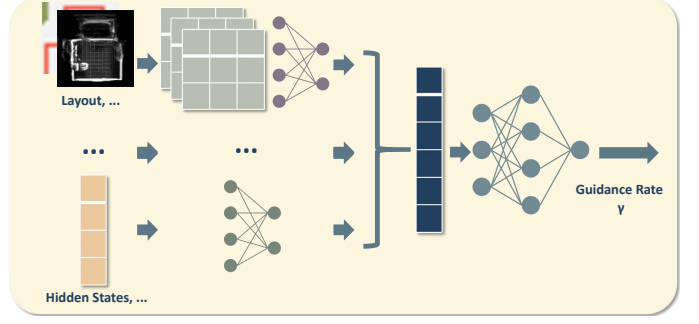


Fig. 2. **Detailed Dynamic Fusion Module Architecture.** The input of the dynamic fusion module could be several environmental and temporal contexts, the encoders of which are dependent on their modalities. All of the flattened features will be further concatenated together before undergoing the final MLP and outputting the guidance rate.

to the specific modality of each context as shown in Fig. 2. For example, if the context is a vector—such as the hidden states of RNN, which inherently represent past experiences—it is processed through a MLP. Conversely, If the context is a matrix—such as a 2D grid map representing the environment layout—it is first encoded with convolutional layers, then flattened into a vector and subsequently processed through a MLP. All available context features are concatenated and fed into the final MLP to obtain the dynamic rate γ . Building on this design, γ is dynamically adjusted according to the context: it decreases in familiar environments where experiential patterns are consistent, and increases in novel or complex settings where LLMs provide more effective navigational insights. This dynamic fusion of affinity scores enables the system to adaptively employ the most effective navigation strategy for the given scenario:

$$A_{F_i} = \gamma \cdot A_{G_i} + (1 - \gamma) \cdot A_{E_i}. \quad (4)$$

Through this mechanism, the dynamic fusion module ensures that the final affinity scores (A_{F_i}) for each object o_i are flexibly adapted to the navigation task’s specific needs. By leveraging both experiential patterns and semantic guidance, the module enhances the agent’s ability to efficiently navigate across diverse environmental contexts, capitalizing on the strengths of both submodules.

D. Integration with Downstream Policy

The LOAT framework’s affinity scores are systematically integrated into downstream policies to intensify the focus on objects pertinent to the navigation goal. This integration applies slightly different strategies for map-based and graph-based policies, optimizing the agent’s navigational efficacy.

Map-based Policy: Let S_m represent a metric map, with each channel assigned to pre-selected object categories, typically large and easily identifiable objects within the environment. The affinity score for each channel c , derived from the dynamic fusion in Equ. (4), is represented by A_{F_c} . The activation of channel c in response to the affinity is computed as:

$$Activation(c) = A_{F_c} \cdot S_m[c]. \quad (5)$$

This channel-wise activation accentuates the channels (object categories) deemed crucial for reaching the goal, enabling a more focused allocation of attention to these areas within the semantic map, thereby facilitating informed navigational decisions.

Graph-based Policy: For a topological graph G , with node N representing a distinct area or a set of objects, let A_{F_N} denote the averaged affinity scores for objects within node N , which is given by:

$$A_{F_N} = \frac{1}{|O_N|} \sum_{o_i \in O_N} A_{F_{o_i}}, \quad (6)$$

where O_N is the object set within node N and $A_{F_{o_i}}$ is the affinity score for object o_i .

Let E_N denotes the embedding for node N . The node activation N is given by:

$$\begin{aligned} \text{Activation}(N) &= E_N \cdot A_{F_N} \\ &= \frac{E_N}{|O_N|} \sum_{o_i \in O_N} A_{F_{o_i}}. \end{aligned} \quad (7)$$

This node-wise activation process highlights nodes with high relevance to the target object, guiding the policy to prioritize exploration of these strategically important nodes.

Training LOAT with Downstream Policy: The original optimization methods for downstream policies can vary, ranging from imitation or reinforcement learning to other training approaches. As long as the training process is gradient-based, LOAT can be integrated with the policy network to facilitate the training process. The training occurs in two phases, using the same dataset as the one employed for training the original policy.

In the first phase, we integrate the experimental affinity module with the base policy and train the entire network using the original loss function. In the second phase, we introduce the generalized affinity module and dynamic fusion layer, updating only the parameters of the dynamic fusion layer while keeping all other parameters frozen.

By employing these strategies, the LOAT framework significantly refines the decision-making process, enhancing the model’s adaptability and generalization capabilities across diverse environments. Through targeted activation within downstream policies, the approach leverages both learned environmental patterns and generalized semantic insights derived from large language models, culminating in a robust framework for focused navigation.

IV. EXPERIMENTS

A. Setup

1) **Benchmarks:** Our methodological evaluation spans across Habitat [10] and AI2-THOR [11] simulators, including three benchmarks emphasizing object goal navigation: Habitat ObjectNav [25], ALFRED [26], and SAVN-NAV¹. Habitat ObjectNav tests agents’ navigation to specified objects in unfamiliar environments using Habitat-Matterport3D scenes

[28]. ALFRED blends navigation with task execution in indoor settings, based on AI2-THOR, focusing on agents’ ability to interpret instructions, navigate to and interact with objects. SAVN-NAV utilizes AI2-THOR for navigation towards 22 target objects within 4 different room types, evaluating inference over 1000 episodes.

2) **Evaluation Metrics:** To rigorously assess our method’s performance across benchmarks, we employ several key metrics: **SR (Success Rate)**: Measures the percentage of episodes where the agent successfully completes the task by reaching the target object. Specifically in ALFRED, it assesses the agent’s effectiveness in both navigating to and engaging with targets to achieve task completion; **SPL (Success weighted by Path Length)**: Defined as the ratio of the shortest path length to the path actually taken by the agent, weighted by whether the episode was successful, evaluating the efficiency of navigation. **PLWSR (Path Length Weighted Success Rate)**: Accounts for the efficiency of the agent’s path towards the target, penalizing longer paths even in successful episodes; **GC (Goal Completion)**: A binary metric indicating whether the agent achieved the task’s objective within the given constraints; **PLWGC (Path Length Weighted Goal Completion)**: Similar to PLWSR, this metric weights the goal completion against the optimality of the path taken; **GFR (Goal Found Rate)**: Specifically introduced for ALFRED to capture instances where the agent locates the target object. It evaluates the method’s precision in guiding the agent to deduce the target’s location from high-level instructions, focusing on navigation success separate from interaction execution.

3) **Implementation Details:** We leverage *paraphrase-MiniLM-L6-v2* [29] to compute text embeddings of category names. This BERT-based model excels in semantic similarity tasks, producing 384-dimensional dense vectors from sentences and phrases, ideal for representing object categories that may extend beyond single words.

To determine object affinities, we consult GPT-4, pre-storing semantic scores for expedited navigation. In cases of open-vocabulary navigation, this process can be executed online at each episode’s onset. This approach is feasible because the maps already have predefined and recognizable large objects to save, with the navigation target being the sole changing factor. When dynamically calculating the guidance ratio γ , we employ two 2-layer MLPs with ReLU activation.

For Habitat ObjectNav, we adopt a model inspired by PEANUT [30] which takes metric maps as inputs and then attempts to predict the locations of target object from incomplete semantic maps and navigating through scripted exploration. This model is trained with the LOAT framework, utilizing pre-generated semantic maps and target distributions. In evaluation of PEANUT enhanced with LOAT, we benchmark against with original PEANUT system and a baseline DD-PPO [31] trained with Behavior Cloning on 20k human demonstrations.

In ALFRED, we enhance the FILM [32] system with LOAT for semantic map activation, replacing MaskRCNN with a fine-tuned DINO [33] model for superior segmentation, and adjusting exploration strategy inspired by Prompter [23] for more efficient navigation. This enhanced system, termed LOAT-P, showcases an integrated approach for improved navi-

¹A benchmark in AI2-THOR collected by Wortsman et. al [27], referred as SAVN-NAV

TABLE II
COMPARISON WITH THE STATE-OF-THE-ART METHODS IN ALFRED.

Method	Tests Seen				Tests Unseen			
	SR	PLWSR	GC	PLWGC	SR	PLWSR	GC	PLWGC
HLSM [34]	29.94	8.74	41.21	14.58	20.27	5.55	30.31	9.99
FILM [32]	27.67	11.23	38.51	15.06	24.46	10.55	36.37	14.30
LGS-RPA [35]	33.01	16.65	41.71	24.49	27.80	12.92	38.55	20.01
EPA [36]	39.96	2.56	44.14	3.47	36.07	2.92	39.54	3.91
Prompter [23]	49.38	23.47	55.90	29.06	42.64	19.49	59.55	25.00
CAPEAM [37]	47.36	19.03	54.38	23.78	43.69	17.64	54.66	22.76
LLM-Planner [24]	18.20	-	26.77	-	16.42	-	23.37	-
LOAT-P (ours)	56.03	28.59	65.36	33.54	54.22	28.12	63.85	33.51

gation and object interaction within AI2-THOR environments. The LOAT-P system is compared with several established methods, including HLSM [34], which employs a spatial-semantic voxel map for environment modeling; FILM [32], recognized for its spatial memory and semantic search capabilities; LGS-RPA [35], which utilizes landmark-guided search; EPA [36], featuring neural-symbolic planning; Prompter [23], which relies on template-based planning; CAPEAM [37], which integrates spatial and state-change information; and LLM-Planner [24], a training-free approach that leverages large language models for few-shot planning.

Additionally, we test the LOAT framework on a graph-based model from the HOZ [4] system in the SAVN-NAV navigation tasks [27], following the original HOZ setup. HOZ models the scene hierarchically with three layers: objects, zones, and scene layers, where each node in the object layer represents a single object, and nodes in subsequent layers encompass object subsets. Node activation scores are calculated as shown in Equation 7. The activated hierarchical graphs are then input into an A3C [38] policy network and trained via reinforcement learning. LOAT-enhanced HOZ is compared to naive A3C navigation policy with a simple visual embedding layer and other graph-centric methods such as ORG [39], and SP [40] that build object semantic relationships.

B. Results

The experiment results in ALFRED are shown in Table II. LOAT-P achieves SOTA performance across all metrics, with a notable 10% increase in SR. Notably, the SR discrepancy between familiar and unfamiliar environments is markedly reduced, showcasing LOAT’s efficacy in applying generalized object affinities from LLM in novel settings. This underscores the system’s robust adaptability and effectiveness across diverse scenarios.

The assessment methodology for SAVN-NAV navigation tasks [27], similar to the HOZ study [4], involves random selection of the agent’s initial position and goal item, with five trials per scenario. Table III displays results for all targets and a subset with optimal path lengths above five steps. Upon integrating the LOAT framework into the HOZ system, we observed improvements in both SPL and SR metrics, surpassing previously reproduced results. This underscores LOAT’s effectiveness within graph-based policy networks.

²We have confirmed with the author that the validation results in the paper are evaluated on 500 episodes from validation set. See this link <https://github.com/ajzhai/PEANUT/issues/3>.

TABLE III
COMPARISON IN SAVN-NAV NAVIGATION TASKS IN AI2-THOR.

Method	All		$L \geq 5$	
	SPL	SR	SPL	SR
Random	1.73	3.56	0.07	0.27
A3C [38](baseline)	33.78	57.35	30.65	45.77
SP [40]	37.01	62.16	34.17	50.86
ORG [39]	38.42	66.38	36.26	55.55
HOZ [4](paper)	40.02	70.62	39.24	62.75
HOZ (reproduced)	38.80	72.20	38.83	64.05
HOZ w/ LOAT	39.56	73.12	39.68	65.26

TABLE IV
RESULTS IN HABITAT OBJECTNAV IN VAL SPLIT.

Method	SPL	SR
DD-PPO [31]	0.20	0.52
Habitat-Web [41]	0.22	0.55
ProcTHOR [42]	0.32	0.54
PIRLNav [43]	0.28	0.62
PEANUT (reproduced)	0.30	0.55
PEANUT w/ LOAT	0.32	0.63
PEANUT (paper) ² [30]	0.32	0.64

Results in validation split of Habitat ObjectNav are shown in Table IV. LOAT improves the reproduced results of PEANUT. Comprehensive analysis across three benchmark evaluations reveals that the LOAT framework excels in three key aspects:

- 1) Improves the effectiveness and adaptability of navigation systems. Systems that leverage LOAT combine experienced object affinities with LLM’s semantic understandings to improve efficiency and generalization, leading to higher success rates, reduced navigation pathways, and improved adaptability to new environments.
- 2) Compatible with various policies. LOAT enhances performance in various navigation contexts by working well with both graph-based and map-based policies, improving performance regardless of the downstream policy mechanism.
- 3) Offers targeted guidance for navigating towards small, hard-to-locate or unseen objects. By leveraging object affinities from both training experiences and LLM insights, it is particularly efficient for detecting objects that are difficult to identify without context from relevant easier-to-find objects.

C. Ablation Studies

1) *Impact of the LOAT Framework in ALFRED [26]:*
The LOAT-P system dramatically increased ALFRED’s per-

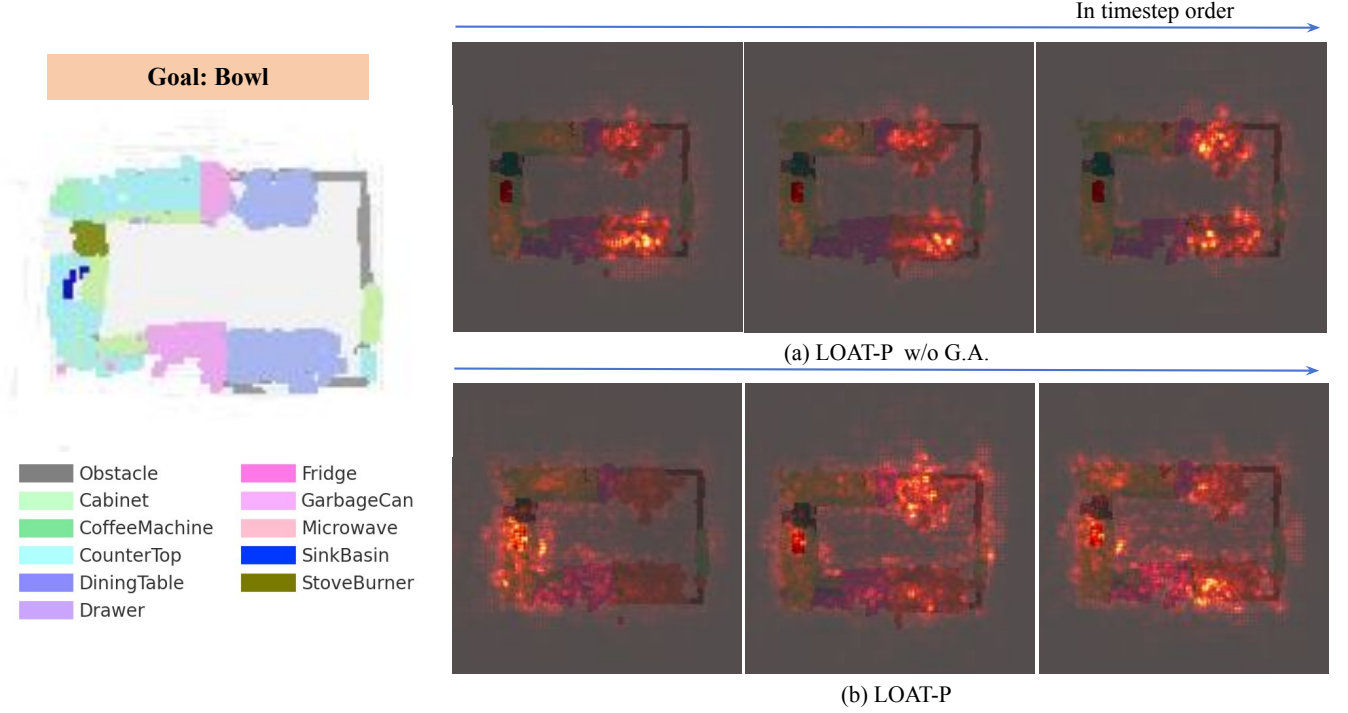


Fig. 3. **Predicted Attention Shifts across Time Steps.** A model without the Generalized Affinities Module tends to fixate on certain areas—such as dining tables when searching for a bowl. In contrast, a model incorporating the full version of LOAT can adapt its focus over time, redirecting attention to other meaningful regions like countertops and sinks.

formance in previous experiments. To differentiate the impact of the LOAT framework from other improvements, such as advanced segmentation methods, LOAT is rigorously evaluated by integrating it into the Prompter [23] and FILM [32] systems within the ALFRED benchmark, while keeping all other variables constant. The outcomes, detailed in Table V, unequivocally show enhancements across all measured metrics upon incorporating the LOAT framework. Notably, the improvement in goal-found rates is a testament to LOAT’s ability to significantly enhance the agent’s proficiency in identifying target objects. This underscores the framework’s effectiveness in augmenting navigational and object-identification capabilities with insights from both LLM-derived object affinities and training-time preferences, thereby contributing to the overall performance uplift.

TABLE V
PERFORMANCE WITH/WITHOUT LOAT FRAMEWORK INTEGRATION IN ALFRED BENCHMARK. WE INTEGRATE THE LOAT FRAMEWORK INTO FILM [32] AND PROMPTER [23] SYSTEMS AND WITNESS CONSISTENT IMPROVEMENTS ACROSS ALL METRICS.

Method	Valid Seen		Valid Unseen	
	SR	GFR	SR	GFR
FILM	20.10	56.15	23.66	58.41
FILM w/ LOAT	22.78 ↑	56.27 ↑	26.46 ↑	60.37 ↑
Prompter	51.04	65.04	52.20	73.66
Prompter w/ LOAT	53.47 ↑	66.63 ↑	53.78 ↑	75.85 ↑

2) *Impact of LOAT Submodules:* The LOAT framework’s integration of Generalized Affinities (G.A.) and Experiential Affinities (E.A.) modules plays a pivotal role in enhancing navigation and task execution, as evidenced by the ablation

study in Table VI. The G.A. module slightly improves success rates, leveraging general knowledge to guide decision-making, but its impact is more nuanced in complex scenarios, suggesting its limitations without learned experience from training environments. Conversely, the E.A. module manages to improve the outcomes in both short and long trials by applying specific past experiences. Additionally, an ablation study of the dynamic fusion module (see supplementary) confirms its effectiveness in adaptively incorporating LLM insights and experiential affinities for goal localization.

The integration of both modules of LOAT framework yields the highest performance improvements. This synergy suggests that while the G.A. module provides a broad knowledge base, the E.A. module extracts targeted knowledge from training time, optimizing the application of both general principles and specific experiences. The comprehensive approach of combining these modules allows the LOAT framework to navigate complex environments more effectively, demonstrating the critical importance of integrating diverse knowledge and experience sources for advanced decision-making and problem-solving capabilities.

In addition to leveraging commonsense from LLMs and experiential object affinities in a parallel manner, we further explore integrating LLM commonsense by employing it as a constraint. Further details can be found in the supplementary materials.

D. Attention Visualization

We employ Grad-Cam [44] to visualize attention within ALFRED’s semantic observations. By treating policy model

TABLE VI
COMPARATIVE EVALUATION OF HOZ INCORPORATING LOAT
FRAMEWORK VARIANTS, EXPERIENTIAL AFFINITIES (E.A.) AND
GENERALIZED AFFINITIES (G.A.) MODULES, INDICATING PERFORMANCE
CHANGES AGAINST THE HOZ BASELINE IN SAVN-NAV NAVIGATION
TASKS [27].

Method	All Trials		Long Trials ($L \geq 5$)	
	SPL (%)	Success (%)	SPL (%)	Success (%)
Baseline (HOZ)	38.80	72.20	38.83	64.05
w/ G.A. Module	38.94 \uparrow	72.40 \uparrow	38.78 \downarrow	64.05 $-$
w/ E.A. Module	39.03 \uparrow	72.51 \uparrow	39.08 \uparrow	64.35 \uparrow
w/ Full LOAT	39.56 \uparrow	73.12 \uparrow	39.68 \uparrow	65.26 \uparrow

outputs as classification targets, we compute gradients against inputted semantic maps, flatten these gradients channel-wise, and visualize them using heat maps overlaid onto flattened semantic maps.

We begin by examining the appropriateness of the attention distribution of different models. As depicted in Fig. 4, the attention distribution in the FILM model is relatively even, highlighting no particular preference for objects. For models incorporating solely the experiential affinities module but no generalized affinities module, as shown in Fig. 4 (b), there’s a notable risk of misdirected attention towards objects commonly encountered in training scenes rather than those with semantic relevance to the target. For example, in Fig. 4, while searching for a piece of cloth, the model inappropriately fixates on a garbage can, prevalent in the training data. However, models guided by generalized object affinities from LLMs successfully realign their focus towards more relevant entities, like a shelf in the given instance, effectively minimizing focus on less pertinent details.

We also investigate the attention transition of models across time steps. As shown in Fig. 3, a model without the Generalized Affinities Module tends to fixate on specific areas, such as dining tables when searching for a bowl. In contrast, a model fully integrated with LOAT exhibits the ability to adjust its focus over time. Initially concentrated on particular features, the model’s attention gradually expands to include additional relevant areas, considering countertops and sinks as guided by LLM feedback. This adaptive attention refinement is particularly beneficial when initial attempts to locate the target fail. It underscores the model’s capacity to dynamically

adjust and optimize its search strategy over time.

E. Evaluation on Out-of-Domain Objects

By utilizing text embeddings instead of one-hot encodings for task representation, we can further examine the model performance over unseen targets in a zero shot manner. The effectiveness of our model in recognizing out-of-domain objects was assessed using 300 pre-collected semantic maps from AI2-THOR environments. We aimed to predict potential locations for unseen target objects based on their category names, involving "Umbrella", "HairDrier", "Scissors", "Toothbrush", "Comb", "Peach", "CanOpener", "Whisk", "Magazine", "Eyeglasses". The model attempts to identify the nearest objects stored in the map to these targets, applying a distance threshold set at one-fifteenth of the map’s total resolution for this experiment. Our primary focus was on assessing the semantic logic behind these probability distributions to determine if the predicted locations for the target objects were plausible within a domestic context. Fig. 5 shows that models relying solely on the experience transfer module may predict a uniform distribution, resulting in semantically incongruous predictions (e.g. associating a can opener with a bathtub basin, which lacks semantic plausibility). LOAT-integrated models better incorporate commonsense reasoning from LLMs, resulting in more logically coherent probability distributions (e.g. placing a can opener near cabinets or coffee tables) reflecting intuitive home placement expectations.

F. Navigation in Real Environments

We deployed the LOAT-P navigation system in two scenes adapted from lab spaces, each designed to represent minimal household environments, featuring typical household objects with clear semantic divisions corresponding to different room types. The system was tasked with searching for five object categories—*Apple, Book, Bowl, and Cup, Laptop*—performing three runs per scene with varying initial positions. Transferred directly from simulation (trained on the ALFRED dataset) to the real world without additional training, the system was deployed on the LoCoBot wx250s. Fig. 6 provides visual examples of the prediction results, demonstrating that the LOAT system is capable of making reasonable predictions in

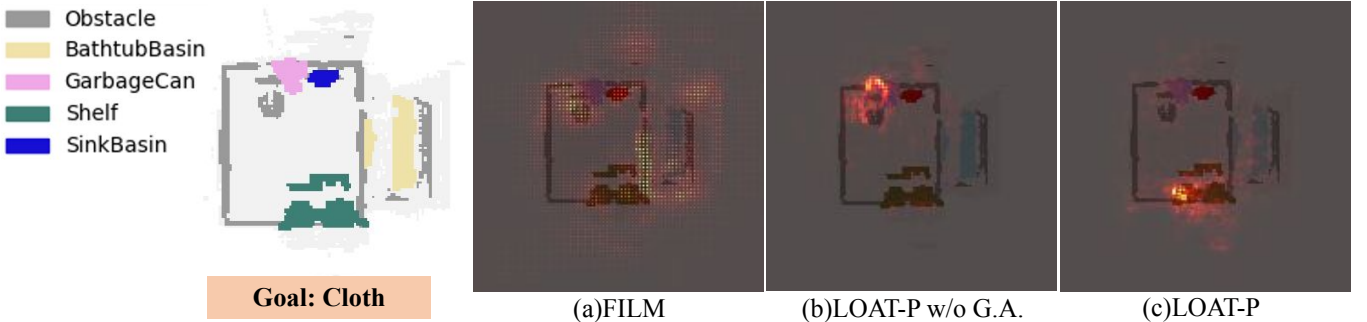
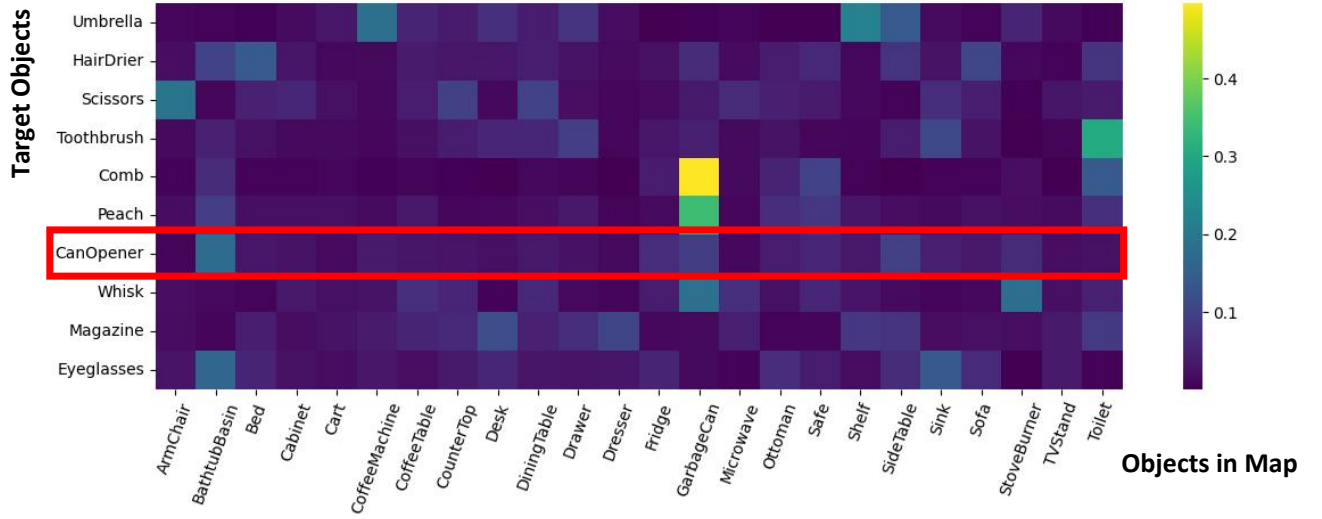
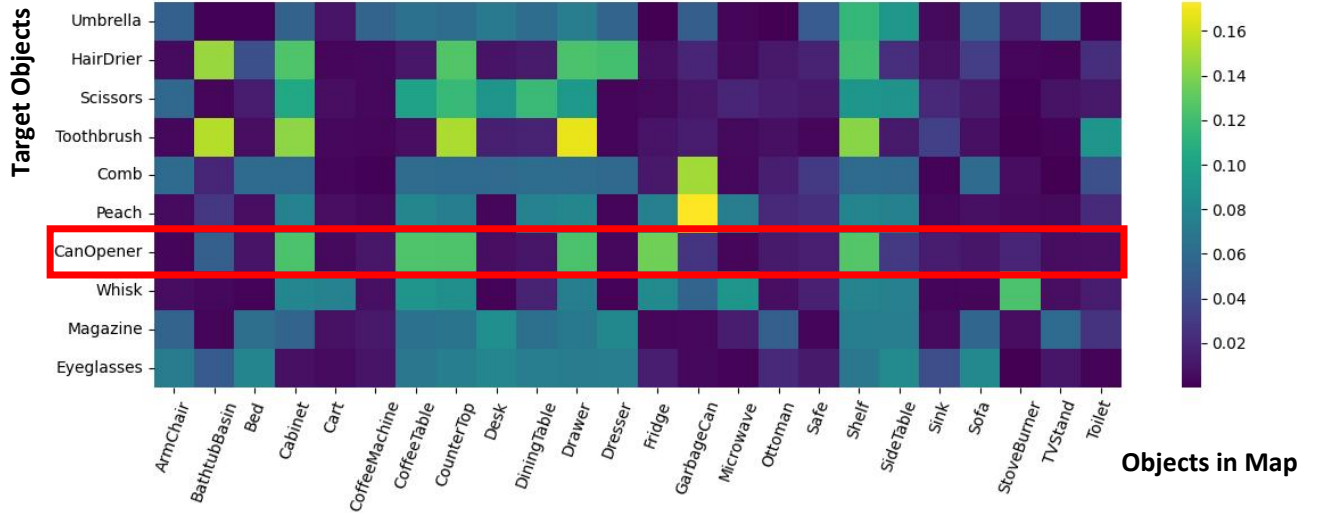


Fig. 4. **Attention Visualization Example.** FILM’s uniform attention distribution lacks object specificity. Models with only Experiential Affinities may emphasize frequent training objects above semantically important ones. In this illustration, it inappropriately accentuates a garbage can, a regular element in training, while searching for cloth. LOAT-enhanced models focus on more appropriate objects like shelves.



(a) LOAT-P w/o G.A.



(b) LOAT-P

Fig. 5. **Predicted Distribution for Out-of-domain Objects.** In subfigure (a), models without the generalized affinities module may make less acceptable assumptions, such as linking a can opener with a bathtub basin. Using LLM-derived knowledge, models in subfigure (b) make more accurate predictions, such as positioning can openers near cabinets or coffee tables.

real-world environments. For instance, when searching for a bowl, the predicted goal position was near the microwave.

In all instances, the robot successfully located the target objects, showcasing the LOAT system’s ability to generalize effectively to previously unseen environments.

V. CONCLUSIONS

This study introduces the LOAT framework, a novel approach that integrates LLM-derived object semantics with historical experiential object affinities to enhance robotic navigation. LOAT significantly improves navigation in environments like AI2-THOR and Habitat across three benchmarks, showing proficiency with unseen objects. It adapts to both metric-map-based and topological-graph-based policies, demonstrating its broad applicability. Visualizations confirm LOAT’s effectiveness in directing policies to focus on semantically relevant ob-

jects and its innovative capacity for dynamic focus adjustment, thereby boosting navigational adaptability and efficiency.

While LOAT’s performance can be influenced by the diversity of object categories in the underlying semantic map, future research could explore extending LOAT’s dual-module strategy to open vocabulary navigation. Such an approach holds promise for expanding its adaptability to a broader range of environments and tasks, further advancing autonomous navigation capabilities.



Fig. 6. **Real-world Navigation Examples.** In real world experiments, model with LOAT was able to make reasonable predictions without extra training.

REFERENCES

- [1] J. Sun, J. Wu, Z. Ji, and Y.-K. Lai, "A survey of object goal navigation," *IEEE Transactions on Automation Science and Engineering*, 2024, DOI:10.1109/TASE.2024.3378010.
- [2] Z. Wang and G. Tian, "Goal-oriented visual semantic navigation using semantic knowledge graph and transformer," *IEEE Transactions on Automation Science and Engineering*, 2024, DOI:10.1109/TASE.2024.3368696.
- [3] J. Chen, G. Li, S. Kumar, B. Ghanem, and F. Yu, "How to not train your dragon: Training-free embodied object goal navigation with semantic frontiers," in *Robotics: Science and Systems XIX, Daegu, Republic of Korea, July 10-14, 2023*, K. E. Bekris, K. Hauser, S. L. Herbert, and J. Yu, Eds., 2023.
- [4] S. Zhang, X. Song, Y. Bai, W. Li, Y. Chu, and S. Jiang, "Hierarchical object-to-zone graph for object navigation," in *Proceedings of the IEEE/CVF international conference on computer vision*, 2021, pp. 15 130–15 140.
- [5] R. Dang, Z. Shi, L. Wang, Z. He, C. Liu, and Q. Chen, "Unbiased directed object attention graph for object navigation," in *Proceedings of the 30th ACM International Conference on Multimedia*, 2022, pp. 3617–3627.
- [6] X. Li, S. Zhang, Y. Lu, K. Dan, L. Ran, P. Wang, and Y. Zhang, "Zero-shot object goal visual navigation with class-independent relationship network," *CoRR*, vol. abs/2310.09883, 2023.
- [7] K. Zhou, K. Zheng, C. Pryor, Y. Shen, H. Jin, L. Getoor, and X. E. Wang, "Esc: Exploration with soft commonsense constraints for zero-shot object navigation," in *International Conference on Machine Learning*, PMLR, 2023, pp. 42 829–42 842.
- [8] A. Rajvanshi, K. Sikka, X. Lin, B. Lee, H.-P. Chiu, and A. Velasquez, "Saynav: Grounding large language models for dynamic planning to navigation in new environments," in *Proceedings of the International Conference on Automated Planning and Scheduling*, vol. 34, 2024, pp. 464–474.
- [9] G. Zhou, Y. Hong, and Q. Wu, "Navgpt: Explicit reasoning in vision-and-language navigation with large language models," in *Proceedings of the AAAI Conference on Artificial Intelligence*, vol. 38, no. 7, 2024, pp. 7641–7649.
- [10] M. Savva, A. Kadian, O. Maksymets, Y. Zhao, E. Wijmans, B. Jain, J. Straub, J. Liu, V. Koltun, J. Malik, D. Parikh, and D. Batra, "Habitat: A Platform for Embodied AI Research," in *Proceedings of the IEEE/CVF International Conference on Computer Vision (ICCV)*, 2019.
- [11] E. Kolve, R. Mottaghi, D. Gordon, Y. Zhu, A. Gupta, and A. Farhadi, "AI2-THOR: an interactive 3d environment for visual AI," *CoRR*, vol. abs/1712.05474, 2017.
- [12] R. C. Smith and P. Cheeseman, "On the representation and estimation of spatial uncertainty," *The international journal of Robotics Research*, vol. 5, no. 4, pp. 56–68, 1986.
- [13] H. Li, Q. Zhang, and D. Zhao, "Deep reinforcement learning-based automatic exploration for navigation in unknown environment," *IEEE Transactions on Neural Networks and Learning Systems*, vol. 31, no. 6, pp. 2064–2076, 2020.
- [14] É. Pairet, J. D. Hernández, M. Carreras, Y. Petillot, and M. Lahijanian, "Online mapping and motion planning under uncertainty for safe navigation in unknown environments," *IEEE Transactions on Automation Science and Engineering*, vol. 19, no. 4, pp. 3356–3378, 2022.
- [15] Y. Chen, X. Zhang, Y. Chen, D. Zhao, Y. Zhao, Z. Zhao, and P. Hu, "Common sense language-guided exploration and hierarchical dense perception for instruction following embodied agents," in *2024 IEEE International Conference on Multimedia and Expo (ICME)*, 2024, pp. 1–6.
- [16] Y. Chen, H. Li, and D. Zhao, "Boosting continuous control with consistency policy," in *Proceedings of the 23rd International Conference on Autonomous Agents and Multiagent Systems, AAMAS 2024, Auckland, New Zealand, May 6-10, 2024*. ACM, 2024, pp. 335–344.
- [17] S. Thrun, "Learning metric-topological maps for indoor mobile robot navigation," *Artificial Intelligence*, vol. 99, no. 1, pp. 21–71, 1998.
- [18] D. S. Chaplot, R. Salakhutdinov, A. Gupta, and S. Gupta, "Neural topological slam for visual navigation," in *Proceedings of the IEEE/CVF Conference on Computer Vision and Pattern Recognition*, 2020, pp. 12 875–12 884.
- [19] D. Li, Q. Zhang, and D. Zhao, "Graph attention memory for visual navigation," in *2022 4th International Conference on Data-driven Optimization of Complex Systems (DOCS)*. IEEE, 2022, pp. 1–7.
- [20] Y. Lu, Y. Chen, D. Zhao, and D. Li, "Mgri: Graph neural network based inference in a markov network with reinforcement learning for visual navigation," *Neurocomputing*, vol. 421, pp. 140–150, 2021.
- [21] A. Topiwala, P. Inani, and A. Kathpal, "Frontier based exploration for autonomous robot," *CoRR*, vol. abs/1806.03581, 2018.
- [22] B. Yu, H. Kasaei, and M. Cao, "L3mvn: Leveraging large language models for visual target navigation," in *2023 IEEE/RSJ International Conference on Intelligent Robots and Systems (IROS)*. IEEE, 2023.
- [23] Y. Inoue and H. Ohashi, "Prompter: Utilizing large language model prompting for a data efficient embodied instruction following," *CoRR*, vol. abs/2211.03267, 2022.
- [24] C. H. Song, J. Wu, C. Washington, B. M. Sadler, W.-L. Chao, and Y. Su, "Llm-planner: Few-shot grounded planning for embodied agents with large language models," in *Proceedings of the IEEE/CVF International Conference on Computer Vision*, 2023, pp. 2998–3009.
- [25] K. Yadav, S. K. Ramakrishnan, A. Gokaslan, O. Maksymets, R. Jain, R. Ramrakhya, A. X. Chang, A. Clegg, M. Savva, E. Undersander, D. S. Chaplot, and D. Batra, "Habitat challenge 2022," <https://aihabitat.org/challenge/2022/>, 2022.
- [26] M. Shridhar, J. Thomason, D. Gordon, Y. Bisk, W. Han, R. Mottaghi, L. Zettlemoyer, and D. Fox, "Alfred: A benchmark for interpreting grounded instructions for everyday tasks," in *Proceedings of the IEEE/CVF conference on computer vision and pattern recognition*, 2020, pp. 10 740–10 749.
- [27] M. Wortsman, K. Ehsani, M. Rastegari, A. Farhadi, and R. Mottaghi, "Learning to learn how to learn: Self-adaptive visual navigation using meta-learning," in *Proceedings of the IEEE/CVF conference on computer vision and pattern recognition*, 2019, pp. 6750–6759.

- [28] S. K. Ramakrishnan, A. Gokaslan, E. Wijmans, O. Maksymets, A. Clegg, J. M. Turner, E. Undersander, W. Galuba, A. Westbury, A. X. Chang, M. Savva, Y. Zhao, and D. Batra, "Habitat-matterport 3d dataset (HM3D): 1000 large-scale 3d environments for embodied AI," in *Proceedings of the Neural Information Processing Systems Track on Datasets and Benchmarks 1*, 2021.
- [29] N. Reimers and I. Gurevych, "Sentence-bert: Sentence embeddings using siamese bert-networks," in *Proceedings of the 2019 Conference on Empirical Methods in Natural Language Processing*. Association for Computational Linguistics, 11 2019. [Online]. Available: <https://arxiv.org/abs/1908.10084>
- [30] A. J. Zhai and S. Wang, "Peanut: predicting and navigating to unseen targets," in *Proceedings of the IEEE/CVF International Conference on Computer Vision*, 2023, pp. 10 926–10 935.
- [31] E. Wijmans, A. Kadian, A. Morcos, S. Lee, I. Essa, D. Parikh, M. Savva, and D. Batra, "DD-PPO: learning near-perfect pointgoal navigators from 2.5 billion frames," in *International Conference on Learning Representations*, 2020.
- [32] S. Y. Min, D. S. Chaplot, P. K. Ravikumar, Y. Bisk, and R. Salakhutdinov, "FILM: following instructions in language with modular methods," in *International Conference on Learning Representations*, 2022.
- [33] M. Caron, H. Touvron, I. Misra, H. Jégou, J. Mairal, P. Bojanowski, and A. Joulin, "Emerging properties in self-supervised vision transformers," in *Proceedings of the IEEE/CVF international conference on computer vision*, 2021, pp. 9650–9660.
- [34] V. Blukis, C. Paxton, D. Fox, A. Garg, and Y. Artzi, "A persistent spatial semantic representation for high-level natural language instruction execution," in *Conference on Robot Learning*. PMLR, 2022, pp. 706–717.
- [35] M. Murray and M. Cakmak, "Following natural language instructions for household tasks with landmark guided search and reinforced pose adjustment," *IEEE Robotics and Automation Letters*, vol. 7, no. 3, pp. 6870–6877, 2022.
- [36] X. Liu, H. Palacios, and C. Muise, "A planning based neural-symbolic approach for embodied instruction following," *Interactions*, vol. 9, no. 8, p. 17, 2022.
- [37] B. Kim, J. Kim, Y. Kim, C. Min, and J. Choi, "Context-aware planning and environment-aware memory for instruction following embodied agents," in *Proceedings of the IEEE/CVF International Conference on Computer Vision*, 2023, pp. 10 936–10 946.
- [38] V. Mnih, A. P. Badia, M. Mirza, A. Graves, T. P. Lillicrap, T. Harley, D. Silver, and K. Kavukcuoglu, "Asynchronous methods for deep reinforcement learning," in *Proceedings of the International Conference on Machine Learning*, 2016, pp. 1928–1937.
- [39] H. Du, X. Yu, and L. Zheng, "Learning object relation graph and tentative policy for visual navigation," *CoRR*, vol. abs/2007.11018, 2020.
- [40] W. Yang, X. Wang, A. Farhadi, A. Gupta, and R. Mottaghi, "Visual semantic navigation using scene priors," in *International Conference on Learning Representations*, 2019.
- [41] R. Ramrakhya, E. Undersander, D. Batra, and A. Das, "Habitat-web: Learning embodied object-search strategies from human demonstrations at scale," in *Proceedings of the IEEE/CVF Conference on Computer Vision and Pattern Recognition*, 2022, pp. 5173–5183.
- [42] M. Deitke, E. VanderBilt, A. Herrasti, L. Weihs, K. Ehsani, J. Salvador, W. Han, E. Kolve, A. Kembhavi, and R. Mottaghi, "Procthor: Large-scale embodied ai using procedural generation," *Advances in Neural Information Processing Systems*, vol. 35, pp. 5982–5994, 2022.
- [43] R. Ramrakhya, D. Batra, E. Wijmans, and A. Das, "Pirlnav: Pretraining with imitation and rl finetuning for objectnav," in *Proceedings of the IEEE/CVF Conference on Computer Vision and Pattern Recognition*, 2023, pp. 17 896–17 906.
- [44] R. R. Selvaraju, M. Cogswell, A. Das, R. Vedantam, D. Parikh, and D. Batra, "Grad-cam: Visual explanations from deep networks via gradient-based localization," *International Journal of Computer Vision*, vol. 128, no. 2, p. 336–359, 2019.

SUPPLEMENTARY MATERIAL

The supplementary material includes an extended ablation study on the dynamic fusion module (Section I), an additional experiment analyzing categorical success rates in Habitat ObjectNav (Section II), an exploration of using LLM commonsense knowledge as a constraint instead of a parallel information source (Section III), additional examples of attention visualization (Section IV), and detailed descriptions of the semantic map formats used in our experiments (Section V).

I. ABLATION ON DYNAMIC FUSION MODULE

We conducted experiments within ALFRED by replacing the dynamic fusion module with fixed guidance rates of 0, 0.5, and 1, with the outcomes detailed in Table I. For clarity, a guidance rate of 0 corresponds to scenarios where the generalized affinities module is omitted, whereas a guidance rate of 1 signifies the exclusion of the experiential affinities module.

TABLE I
PERFORMANCE WITH DIFFERENT GUIDANCE RATE SETTINGS IN ALFRED BENCHMARK. MODEL HAVING A DYNAMIC FUSION MODULE IS DENOTED BY *Dynamic*, WHILE THE REST ARE MODELS WITH FIXED GUIDANCE RATES.

Guidance Rate	Valid Seen		Valid Unseen	
	SR	GFR	SR	GFR
0	61.22	91.83	62.00	87.21
0.5	62.71	92.55	59.95	87.42
1	60.37	92.07	60.41	87.58
Dynamic	59.15	92.56	63.22	90.13

Analyzing the experimental results shown in Table I, we observe that the dynamic fusion module distinctly enhances the GFR, especially in unseen environments. This emphasizes the module’s ability to effectively assist in locating navigation goals, highlighting the importance and effectiveness of dynamic adaptation in processing LLM insights and historical affinities.

With fixed guidance rates, we see that while SR might fluctuate, the dynamic fusion approach consistently achieves higher GFR, indicating superior performance in identifying target objects. This advantage does not always translate into higher SR, potentially due to interaction execution failures within the AI2-THOR simulator. Particularly in unseen settings, the model with dynamic fusion outperforms the fixed-rate configurations, suggesting its superior capacity to generalize and apply learned and inferred object affinities to novel situations.

II. CATEGORY-WISE ANALYSIS OF SUCCESS RATES

As detailed in Table II, we conducted a categorical analysis of success rates across different object types. Notably, our approach has significantly enhanced the success rate for locating smaller, hard-to-find objects, such as ‘plant,’ which often pose challenges due to their size and positioning in complex environments. This improvement highlights the model’s capacity to handle diverse navigation demands, particularly for smaller, less prominent objects that are typically challenging to detect and approach accurately.

However, certain categories, like ‘Chair’ and ‘Sofa,’ exhibited lower success rates. This can be partially attributed to the limitations of the semantic maps used, as the PEANUT setting [?] only includes nine object categories, compared to over 20 in the ALFRED [?] benchmark. The restricted object diversity in PEANUT may hinder the model’s ability to fully capitalize on its capabilities.

TABLE II
SUCCESS RATES BY CATEGORY IN HABITAT OBJECTNAV

Category	PEANUT (reproduced) [?]	PEAUT w/ LOAT
Chair	0.78	0.68
Bed	0.54	0.57
Plant	0.11	0.32
Toilet	0.58	0.60
TV Monitor	0.41	0.42
Sofa	0.71	0.64

III. COMPARATIVE ANALYSIS OF LLM INTEGRATION STRATEGIES FOR LOAT

Building on the previously introduced method, we further explore integrating LLM commonsense by employing it as a constraint, differing from its parallel use as an information source. This exploration led to the development of two distinct designs: LOAT-AVG, the design we use throughout previous sections, where experiences from both sources are averaged, and the newly introduced LOAT-MUL, which uses a multiplicative attention mechanism. In LOAT-MUL, embeddings for target and environmental objects serve as queries and keys. The values, determined by the semantic proximity as per the prior knowledge of large language models, are assigned such that objects semantically close to the target are emphasized (assigned a value of 1), while others are de-emphasized (assigned a value of 0).

The mathematical formulation is as follows, employing the same notation introduced in the *Method* section. We derive key queries by transforming embeddings of the target and environmental object categories. The values are the semantic relevance of each object o_i in the map to the target o_{target} , represented by a binary value $S(o_i, o_{target})$ determined by the LLM. The output of the LOAT-MUL attention mechanism, A_{MUL_i} for each object o_i , is then calculated as:

$$A_{MUL_i} = S(o_i, o_{target}) \cdot \frac{\exp(\mathbf{Q} \cdot \mathbf{K}^T / \sqrt{d_k})}{\sum_{j=1}^M \exp(\mathbf{Q} \cdot \mathbf{K}_j^T / \sqrt{d_k})}. \quad (1)$$

This method uses LLM knowledge as a gating mechanism to refine attention by emphasizing objects that are closely connected to the objective and ignoring all other objects that are judged irrelevant. Comparative results between the two LOAT designs in the ALFRED benchmark are detailed in Table III. LLM-AVG-P exhibits higher goal found rates (GFR) in both seen and unseen scenarios compared to LOAT-MUL-P, despite achieving lower success rates (SR). This discrepancy may result from interaction execution failures (e.g. Fail to pick up objects.) within the AI2-THOR simulator environment. Although overall performance between the two methods is similar, LLM-AVG-P demonstrates a slight advantage in

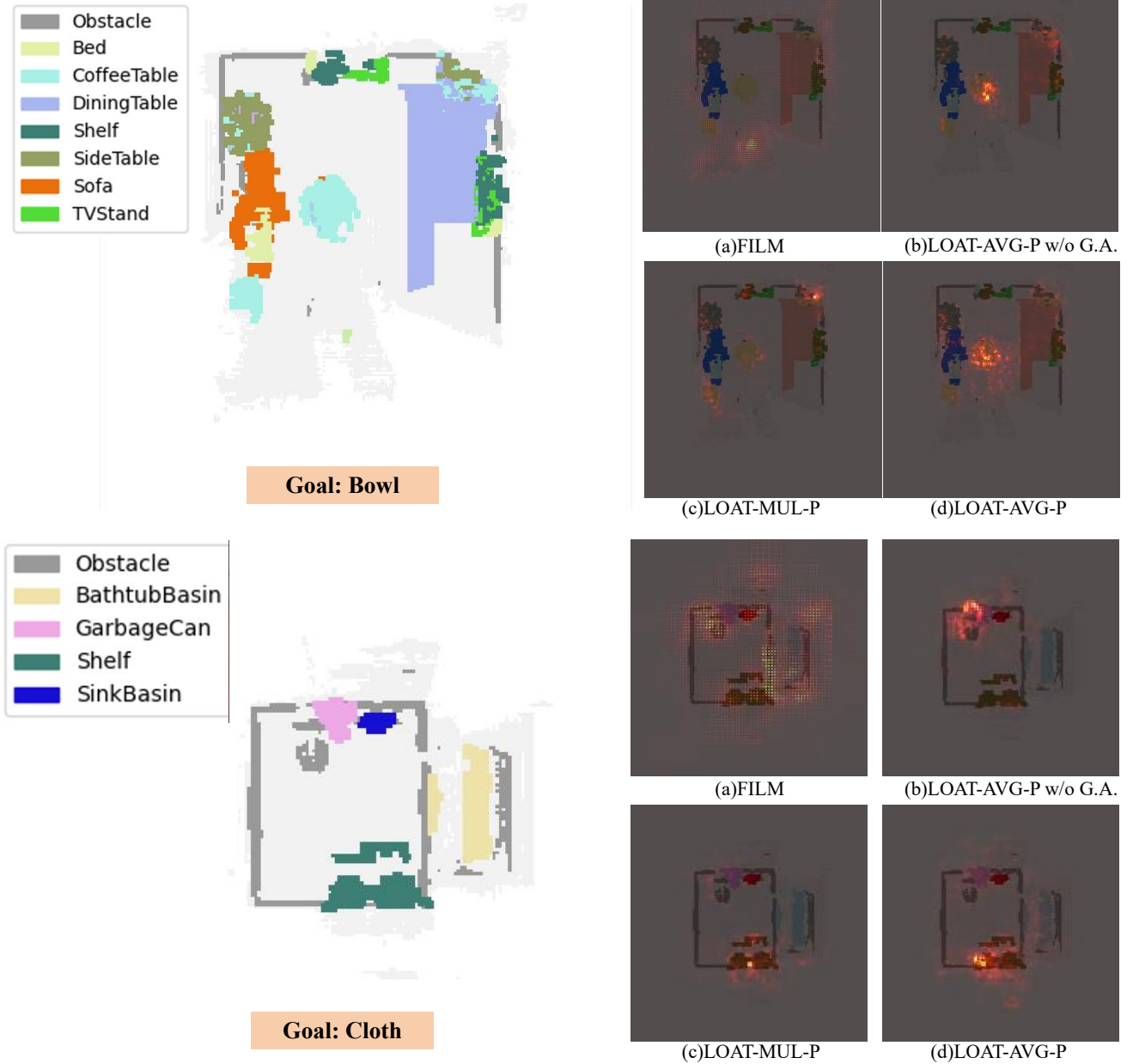


Fig. 1. **Attention Visualization Examples.** LOAT-MUL models have more selective focus compared with LOAT-AVG models.

target object localization. This advantage likely arises from LOAT-MUL-P’s gating mechanism, which may inadvertently overlook objects with subtle yet significant associations. In contrast, LLM-AVG-P maintains a more nuanced understanding of object relationships by averaging direct object affinities with LLM guidance, thereby enabling a more comprehensive attention allocation.

TABLE III
PERFORMANCE WITH DIFFERENT LOAT FRAMEWORK DESIGNS IN ALFRED BENCHMARK. LOAT-AVG-P IS THE LOAT-P REFERRED IN PREVIOUS CONTEXT. LOAT-MUL-P USES LOAT-MUL TO REPLACE THE ORIGINAL LOAT-AVG DESIGN IN THE LOAT-P SYSTEM.

Method	Valid Seen		Valid Unseen	
	SR	GFR	SR	GFR
LOAT-MUL-P	59.51	91.83	63.93	90.01
LOAT-AVG-P	59.15	92.56	63.22	90.13

IV. MORE ATTENTION VISUALIZATION EXAMPLES

We also utilize the same approach as described in *Attention Visualization* section to display the attention for models with LOAT-MUL. As previously noted, the attention distribution in the FILM model is notably uniform, lacking focused areas that signify object preference. However, the LOAT framework significantly sharpens models’ focus on objects with semantic relevance, reducing attention to extraneous details.

This section delves deeper into the comparison between LOAT-MUL and LOAT-AVG models. As depicted in Fig. 1, LOAT-MUL models employ LLM-derived common-sense knowledge as a stringent filter and achieve a more focused attention. However, this selective focus can sometimes lead to the omission of objects with subtle but meaningful associations. For the LOAT-AVG models, which synthesize

insights from both commonsense knowledge and experience transfer through a weighted average, exhibit a more balanced attention distribution. his approach allows for a nuanced understanding by preserving objects of marginal relevance acquired during training. Such a balance enhances the model’s ability to retain potentially important objects that might not be immediately apparent, supporting a more comprehensive and adaptive attention strategy

V. SEMANTIC MAP FORMAT DETAILS

This section outlines the semantic map formats utilized in our navigation task experiments across three benchmarks:

ALFRED [?] Benchmark: Our approach adopts the FILM [?] model setup, leveraging metric maps with a shape of (24, 240, 240). This configuration signifies the inclusion of 24 object categories within a 240x240 resolution map.

SAVN-NAV [?] Navigation Task: Building on the HOZ [?] framework, our model integrates hierarchical object-to-zone graphs encompassing object, zone, and scene layers. Specifically, in room-wise HOZ graphs, zone nodes are derived from clustering egocentric observation features, with edges representing the adjacency likelihood between zones—this probability echoes the co-occurrence rate of objects within zones. Subsequently, room-wise HOZ graphs are amalgamated into comprehensive scene-wise graphs for a holistic environmental depiction.

Habitat ObjectNav [?] Benchmark: Aligning with the PEANUT [?] model, our system employs metric maps of shape (9, 960, 960), which account for 9 object categories within a high-resolution 960x960 map.